Tetrahedron Letters 53 (2012) 931–935

Contents lists available at SciVerse ScienceDirect

Tetrahedron Letters

journal homepage: www.elsevier.com/locate/tetlet

Deuteration of molecules for neutron reflectometry on organic light-emitting diode thin films

Tamim A. Darwish [a,*], Arthur R.G. Smith [b], Ian R. Gentle [b,c], Paul L. Burn [b], Emily Luks [a], Greta Moraes [a], Marie Gillon [a], Peter J. Holden [a], Michael James [a,d,*]

[a] National Deuteration Facility, Bragg Institute, Australian Nuclear Science and Technology Organisation, Locked Bag 2001, Kirrawee DC, NSW 2232, Australia
[b] Centre for Organic Photonics & Electronics, The University of Queensland, Brisbane, QLD 4072, Australia
[c] School of Chemistry and Molecular Biosciences, The University of Queensland, Brisbane, QLD 4072, Australia
[d] School of Chemistry, The University of New South Wales, Kensington, NSW 2052, Australia

ARTICLE INFO

Article history:
Received 12 October 2011
Revised 27 November 2011
Accepted 9 December 2011
Available online 16 December 2011

Keywords:
Hydrothermal deuteration
Aromatic heterocycles
Steric availability
Organic light-emitting diode
Neutron reflectometry

ABSTRACT

Deuterated forms of aromatic charge transporting heterocycles **2** and **3** used in organic light-emitting diodes have been produced by hydrothermal reactions, catalyzed by Pt/C or Pd/C. Comprehensive analysis by mass spectroscopy, ^{1}H, ^{2}H and ^{13}C NMR enables determination of the overall quantity of D atoms present, as well as the level of deuteration at each molecular site. The roles of solubility and steric availability in deuteration are discussed in the light of these results. Neutron reflectometry indicates excellent scattering contrast between protonated and deuterated forms of these molecules, with nanoscale thin films showing the same density as in their bulk molecular forms. Although used for morphological studies of thin films typically used in OLEDs, the synthetic and analysis methods described here are generic and suitable for deuteration of other conjugated aromatic heterocycles and other optoelectronic devices.

Organic optoelectronics is a rapidly growing area of interdisciplinary science and technology, with investigations focused on both small molecules,[1,2] conjugated polymers,[3a] and dendrimers[3b,c] that can be used as the light-emitting layers in organic light-emitting diodes (OLEDs). A fundamental feature of these devices is that they are comprised of more than one layer and hence rely on electron transfer processes at interfaces. Conjugated aromatic heterocycles such as **2** and **3** (Fig. 1) are widely used electron and hole transport materials, respectively. The current generation of OLEDs, having internal quantum efficiencies of ~100%, are based on small molecule phosphorescent iridium(III) complexes [e.g., *fac*-tris(2-phenylpyridyl)iridium(III) ($Ir(ppy)_3$] blended with an organic host material [e.g., 4,4′-bis(*N*-carbazolyl)biphenyl (CBP)] in the emissive layer.[2] While efficiencies of these layered devices are very high, their lifetimes depend on a range of factors including the morphological stability of layers in the device.[4] Investigations of functioning devices with buried interfaces present numerous difficulties using conventional surface science techniques and so neutron reflectometry along with selective deuteration has become the key method for the study of morphology, diffusion, and interfacial behavior in organic thin-film semiconducting devices.[5] Selective deuteration of these aromatic and heterocyclic molecules leads to a substantial increase in neutron scattering length density compared to their equivalent protonated forms. In addition to such morphological studies, recent investigations have also centered on isotope effects associated with deuterium that lead to substantial increases in the quantum efficiency and high-voltage stability of Al-based[5j] and Ir-based[5k] OLEDs.

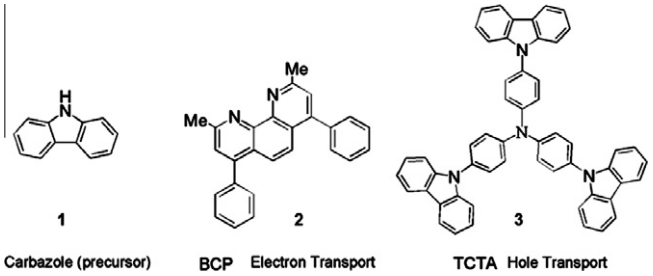

Figure 1. OLED molecules **2** and **3** and precursor **1**.

There have been a number of studies detailing different methods for synthesizing deuterated aromatic and heterocyclic compounds; these being ably summarized by the early work of Hawthorne et al.[6] and recent published works of Derdau, Atzrodt, and co-workers,[7] as well as numerous studies by Sajiki et al.[8] This Letter reports the deuteration of molecules that form key components of the electron and

* Corresponding authors.
E-mail address: tde@ansto.gov.au (T.A. Darwish).

0040-4039/$ - see front matter Crown Copyright © 2011 Published by Elsevier Ltd. All rights reserved.
doi:10.1016/j.tetlet.2011.12.032

hole transport layers of an OLED device, and assesses the synthetic outcomes in light of different deuteration conditions. The role of solubility and steric availability of proton sites is also discussed. Finally, results from the application of these deuterated molecules in the study of interfacial morphology of films typically applied in OLEDs using neutron reflectometry are presented.

Deuteration of the molecules presented in this study was achieved either by H/D exchange reactions with deuterium oxide catalyzed by Pt/C and Pd/C under hydrothermal conditions, or by synthesis from deuterated precursors produced by the same method. Sajiki et al. have demonstrated that platinum catalysts generally have a higher tendency toward the deuteration of aromatic positions, whereas palladium catalysts preferentially deuterate aliphatic positions.[8i] The same authors also showed that Pt/C and Pd/C when used together have a synergistic effect in deuterating sterically hindered aromatic positions.[8j] It is known that this method is dependent on both electronic and steric factors, and it has been suggested that the high affinity of Pt or Pd metal for a nitrogen lone pair increases the efficiency of the exchange reaction.[8e] Lower incorporation of deuterium has been observed on groups neighboring sterically encumbered nitrogen atoms. For our study, the optimized conditions, overall yield and deuteration outcomes are summarized in Table 1.

Carbazole-d_8 (**1**) was the most efficiently produced molecule in this study under hydrothermal conditions (240 °C), which was performed on ca. 10 g scale and gave 80% yield and 94% deuteration of the aromatic proton sites (Supplementary data, Figs. S1–S3). This is attributed to the high solubility of carbazole in D_2O at elevated temperatures and the lack of steric crowding of its proton sites.

Although prepared at a lower temperature (180 °C) than **1**, the optimized hydrothermal deuteration of BCP-d_{20} (**2**) gave a poorer yield (50%) and lower deuteration levels. The broad isotope cluster shown in the ESI-MS spectrum of BCP-d_{20} (Fig. 2) indicates a distribution of protonated and deuterated sites within the molecule (incomplete deuteration). The analysis of the area under these peaks in the spectrum suggests an average of 68% deuteration. The presence of the signal m/z: 361, which corresponds to the completely non-deuterated species (i.e., d_0), separate from the continuous isotope cluster (d_{11}–d_{20}) suggests solubility issues. Material that remained insoluble is expected to stay non-deuterated, while the material that dissolved in the solution incorporated deuterium atoms and formed a continuous mass distribution envelope (d_{11}–d_{20}). The combination of ^{1}H, ^{2}H and ^{13}C NMR spectra (Supplementary data, Figs. S4–S8) allowed us to confirm the total deuterium content for this molecule, but also importantly, gives a clear indication of the relative occurrence of hydrogen and deuterium atoms at specific sites within the molecule.

The percentage protonation of residual signals for individual ^{1}H resonances within the molecule was determined by ^{1}H NMR spectroscopy (Supplementary data, Fig. S4) using a protonated internal standard (i.e., MeOH). ^{2}H NMR spectroscopy confirmed the deuteration at these positions by showing reciprocal resonances for each deuterated position (Supplementary data, Fig. S5), whereas ^{13}C NMR spectroscopy allowed observation of the deuterated and protonated extent at each position simultaneously, utilizing the secondary isotope effect on the observed ^{13}C nucleus.[9] The latter was achieved by running an inverse gated ^{13}C NMR experiment with long delays between pulses (i.e., D_1 = 20 s); observing ^{13}C nuclei while decoupling both ^{1}H and ^{2}H nuclei. This technique is a particularly useful analysis tool, as experiments can be designed that discriminate between resonances of the various types of carbons present: fully deuterated groups (CD, CD_2, CD_3), partially deuterated groups (CHD, CHD_2, CH_2D), and non-deuterated groups (C, CH, CH_2, CH_3). By comparing the ^{13}C{^{1}H, ^{2}H} (decoupling both ^{1}H and ^{2}H) spectrum to the normal ^{13}C{^{1}H} (proton decoupled only) NMR, it was possible to differentiate between carbons with and without deuterons. This allowed the determination of the percent deuteration at specific sites in the molecule, as shown in Figure 3, and confirmed the percent deuteration obtained from ^{1}H NMR analysis with an internal standard, the values agreeing to within ±1%. Additionally, this technique allowed determination of the percent deuteration at carbon positions where the corresponding residual proton resonances overlap in the ^{1}H NMR spectrum. For example, in BCP (2,9-dimethyl-4,7-diphenyl-1,10-phenanthroline), the residual protons at the *ortho*, *meta*, and *para* positions of the two phenyl groups at position C(3) (Fig. 3) have overlapping resonances in the ^{1}H NMR spectrum, while their three carbon resonances in the ^{13}C NMR spectra are well resolved (Supplementary data, Fig. S8).

Of the 20 protons available within BCP, six distinct sites are evident (Fig. 3) which were found to be deuterated to different degrees depending on the steric hindrance and availability of these sites for H/D exchange with the catalyst. Methyl protons at the C(1) position showed the highest deuteration levels (90%), while protons at the C(2) position showed only 40% deuteration due to the steric shielding from the phenyl groups. The *ortho*-, *meta*-, and *para*-positions on the two phenyl groups at position C(3) in Figure 3 were found to be deuterated at 55%, 86%, and 90%, respectively. The remaining two protons attached to the phenanthroline moiety at position C(4) are strongly sterically shielded by the pendant phenyl groups, such that the catalyst had restricted access to these positions and hence they were deuterated at the 4% level.

Attempts at producing TCTA-d_{36} [tris(4-carbazoyl-9-ylphenyl)amine-d_{36}] using hydrothermal methods and a similar approach to that used for **1** produced either no deuteration at 240 °C, or substantial decomposition (30% yield) and poor deuteration (15% D) at 265 °C (Supplementary data, Fig. S9). The lack of deuteration at lower temperatures appears to be correlated to the poor solubility of TCTA in D_2O.

Table 1
Optimized hydrothermal reaction conditions for **1**–**3**

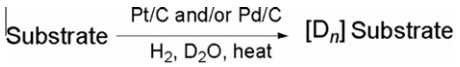

Reagents/catalyst	Temp. (°C)	Time (h)	Composition/average % deuteration	Yield (%)
Carbazole (59.8 mmol), D_2O (120 mL), Pt/C (2.5 g)	240	48	$C_{12}D_8HN$ (**1**) 94%	80
BCP (1.38 mmol), D_2O (35 mL), Pt/C (0.25 g)	180	96	$C_{26}D_{14}H_6N_2$ (**2**) 68%	50
TCTA (0.67 mmol), D_2O (30 mL), THF (10 mL), Pt/C (0.23 g), Pd/C (0.23 g), H_2 (1 L)	140	18 × 3[a]	$C_{54}D_{15}H_{21}N_4$ (**3**) 42%	56

[a] Products were extracted and analyzed after each run, before returning to the Parr reactor with fresh reagents and catalysts.

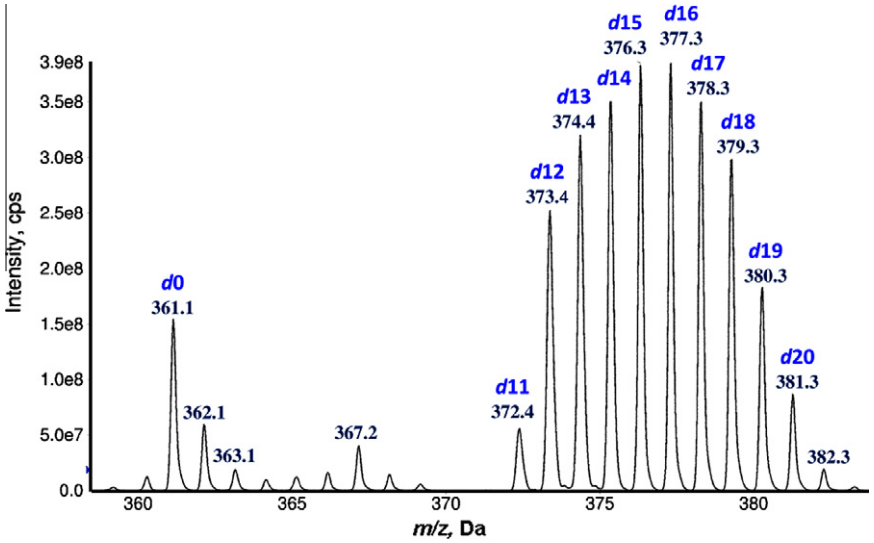

Figure 2. ESI-mass spectrum (+ve ER) for partially deuterated BCP-d_{20} (**2**).

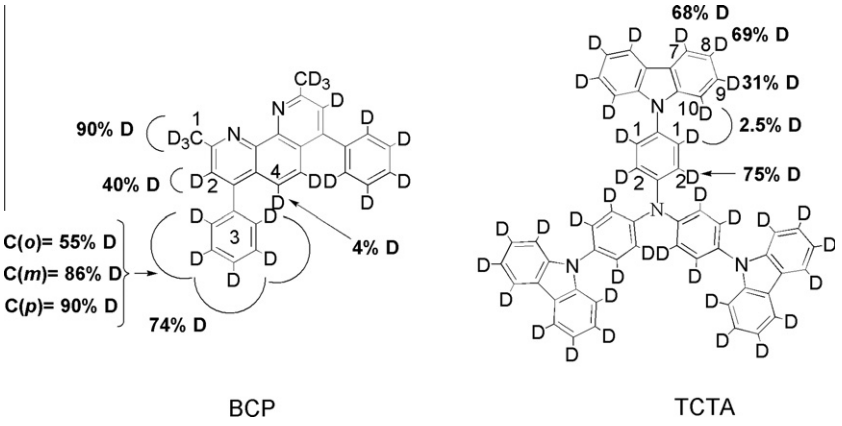

Figure 3. Site-specific deuteration levels for BCP-d_{20} (**2**) and TCTA-d_{36} (**3**).

Addition of THF as a co-solvent to the reaction solution improved the solubility of TCTA and allowed significant deuteration under hydrothermal conditions. A similar approach of using THF as a co-solvent has also been shown to be effective by Sajiki and co-workers[8g] to deuterate estrogen under conditions where solubility in D_2O was relatively poor. The isotopic distribution shown in the ESI-MS spectrum of TCTA-d_{36} (Fig. 4) indicates a distribution of protonated and deuterated sites, and analysis of the area under the peaks shows increasing deuteration levels of 27%, 35%, and 42% after reaction for 1, 2, and 3 days, respectively. The fully protonated form of TCTA-h_{36} in this plot shows a peak at m/z = 740; while per-deuterated TCTA-d_{36} gives an m/z peak of 776. The shift of the mass distribution envelope to a higher mass (to the right) indicates higher deuterium content after each cycle. Characterization of TCTA-d_{36} (**3**; after 3 days) using NMR confirmed the overall deuteration level (Supplementary data, Figs. S10–S13) and again allowed the assignment of deuteration levels at specific sites (Fig. 3). ^{1}H NMR spectroscopic resonances associated with positions C(7), C(8), and C(9) on the carbazole pendants were well resolved, and showed deuteration levels of 68%, 69%, and 31%, respectively (Fig. 5). ^{1}H resonances associated with positions C(1), C(2), and C(10) overlap so their individual contributions could not be accurately assigned (Supplementary data, Fig. S10), but as a group these three positions showed an average deuteration level of 27%. Subsequently, ^{13}C NMR (Supplementary data, Figs. S12–S13) was used to help discriminate between these three sites. Analysis of the data showed that site C(2) was 75% deuterated, thus indicating that very little deuteration (<3% on average) had taken place at the sterically hindered sites C(1) and C(10).

Due to the poor yields and relatively low total deuteration level of TCTA-d_{36} (**3**) by hydrothermal methods, another form of the molecule (TCTA-d_{24} **3b**) was synthesized using the highly deuterated carbazole-d_8 (**1**) and protonated tris(4-bromophenyl)amine via a modified Ullman condensation[10] (Supplementary data, Section 1.3). Analysis of the product **3b** (80% yield) using ESI-MS and NMR spectroscopy confirmed the expected 63% overall deuteration level, with the protonated triphenylamine core and essentially per-deuterated carbazole pendant groups (Scheme 1). Compound **3b** was subsequently used to produce thin film samples for study using neutron reflectometry.

Thin films of the desired protonated and deuterated compounds were prepared by thermal evaporation under high vacuum onto silicon wafers, and neutron reflectivity measured using the Platypus time-of-flight neutron reflectometer at the OPAL 20 MW research reactor [Australian Nuclear Science and Technology Organisation (ANSTO), Sydney, Australia].[11] Further details of the neutron reflectometry experiment are given in the Supplementary data (Section 2). Very good fits to observed neutron reflectivity data were obtained from films of TCTA-d_{24} (**3b**; Supplementary data, Fig. S19) and BCP-d_{20} (**2**; Fig. S20) using the MOTOFIT analysis

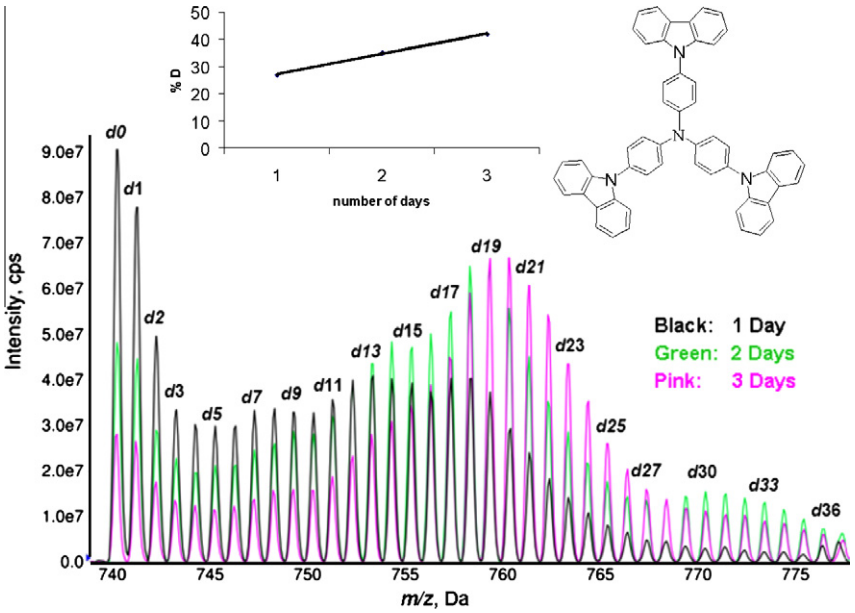

Figure 4. ESI-mass spectra for TCTA-d_{36} as a function of reaction time with fresh THF/D_2O mixture each cycle.

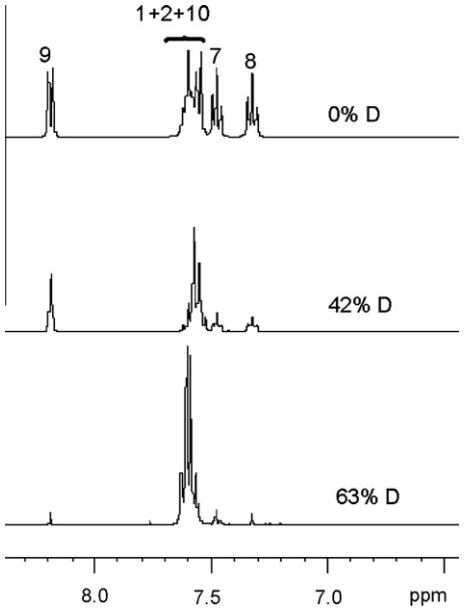

Figure 5. ^1H NMR (CD_2Cl_2, 400 MHz) spectra (from top to bottom) of TCTA-h_{36}, TCTA-d_{24} (**3**) deuterated using a hydrothermal method and synthesized TCTA-d_{24} (**3b**) from deuterated carbazole and protonated tris(4-bromophenyl)amine.

software[12] and single layer models. Refined structural data indicate high-quality films of thickness 168(1) Å and 185(1) Å, respectively, surface roughness less than 1 nm, and scattering length density (SLD) values of $4.83(3) \times 10^{-6}$ Å^{-2} and $5.02(4) \times 10^{-6}$ Å^{-2}. These values are important, as they indicate that films of TCTA-d_{24} and BCP-d_{20} have the same mass density as their bulk protonated forms.

Analysis of neutron reflectivity data (Fig. 6) from a bilayer film formed by a 420(1) Å thick layer of protonated Ir(ppy)$_3$:CBP (a typical light-emitting blend layer) deposited onto a 279(1) Å thick base layer of TCTA-d_{24} (**3b**) shows excellent scattering contrast between the two layers (SLD = $2.46(3) \times 10^{-6}$ Å^{-2} and $4.83(4) \times 10^{-6}$ Å^{-2}, respectively). The SLD values of each layer in this bilayer film are essentially the same as those observed for the individual single layer films. Excellent contrast was also observed for the (TCTA-d_{24})/Ir(ppy)$_3$:CBP/(BCP-d_{20}) multilayer film used in our study of interfacial diffusion.[5h] In that study, the three layer structure was found to be stable at temperatures up to 60 °C.

At 100 °C however, the Ir(ppy)$_3$:CBP and BCP-d_{20} layers were found to intermix; while the (TCTA-d_{24})/Ir(ppy)$_3$:CBP interface remained stable with no diffusion taking place. Without the availability of BCP-d_{20} and TCTA-d_{24} such a study would not have been possible. Protonated forms of BCP and TCTA in these thin-film devices would not have provided adequate scattering contrast between the CBP emissive layer (SLD = 2.46×10^{-6} Å^{-2}); the BCP

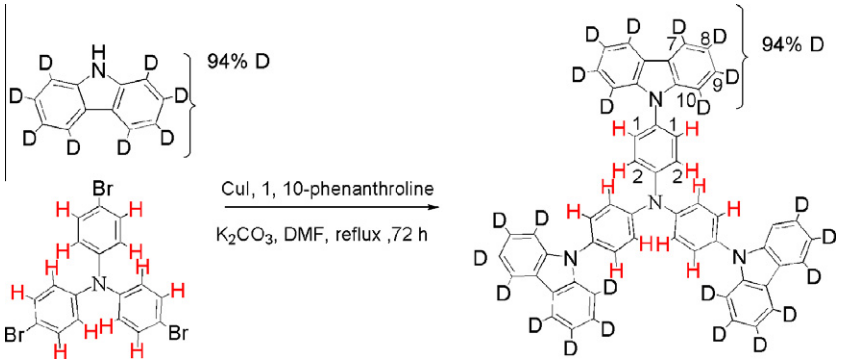

Scheme 1. Synthesis of TCTA-d_{24} (**3b**).

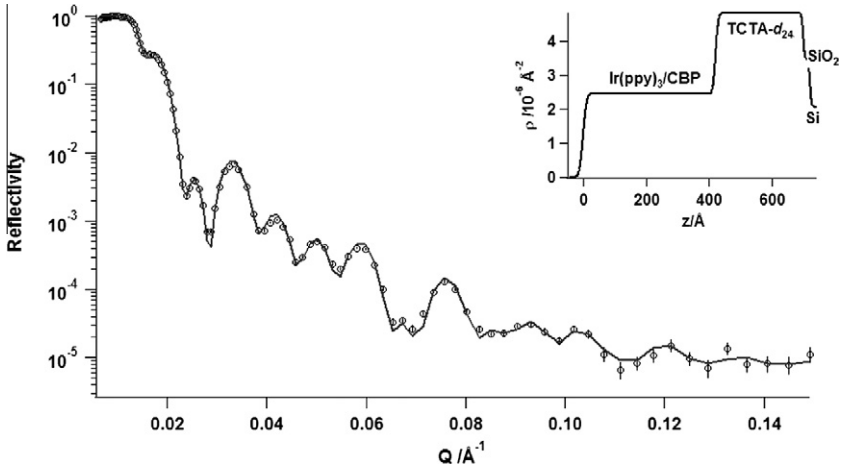

Figure 6. Observed (points) and calculated (solid line) neutron reflectometry profiles for a TCTA-d_{24}/Ir(ppy)$_3$:CBP bilayer film on Si. Inset shows the SLD profile.

layer having an SLD of $\sim 2.3 \times 10^{-6}$ Å^{-2} and the TCTA layer with an SLD of $\sim 2.6 \times 10^{-6}$ Å^{-2}.

In conclusion, we have produced relatively large quantities of deuterated materials typically used in OLEDs using hydrothermal conditions with Pt/C and Pd/C as catalysts. In the case of BCP, the availability of two nitrogen atoms which can coordinate to the metal catalyst increases its accessibility and thus enhances the H/D exchange process. The hydrothermal exchange reaction with insoluble TCTA was only achieved by using protonated THF as a co-solvent. The extent of deuteration in each case was estimated using a combination of ESI-MS, ^{1}H, ^{2}H, and ^{13}C NMR analysis which showed lower deuteration percentages at sites associated with steric hindrance and low accessibility for the catalyst. The use of inverse gated ^{13}C NMR experiments were particularly useful in decoupling overlapping ^{1}H resonances from multiple sites, giving unique assignment of site-specific deuteration levels. These synthetic and characterization results show the ability for these techniques to be used in the deuteration of other conjugated aromatic heterocycles. Neutron reflectometry measurements indicate smooth, fully dense molecular films with excellent scattering contrast between the protonated and deuterated components.

Acknowledgments

Synthesis of the molecules described here was conducted at the National Deuteration Facility and was partly supported by the National Collaborative Research Infrastructure Strategy—an initiative of the Australian Government. A.R.G.S. would like to thank the Australian Institute of Nuclear Science and Engineering for a postgraduate research award. P.L.B. is a recipient of an Australian Research Council Federation Fellowship (Project no. FF0668728). We acknowledge funding from the University of Queensland (Strategic Initiative-Centre for Organic Photonics & Electronics).

Supplementary data

Supplementary data (synthesis, NMR and MS spectroscopy characterization and spectra and the neutron reflectometry details) associated with this article can be found, in the online version, at doi:10.1016/j.tetlet.2011.12.032.

References and notes

1. Tang, C. W.; Van Slyke, S. A. *Appl. Phys. Lett.* **1987**, *51*, 913.
2. (a) Adachi, C.; Baldo, M. A.; Thompson, M. E.; Forrest, S. R. *J. Appl. Phys.* **2001**, *90*, 5048; (b) Ikai, M.; Tokito, S.; Sakamoto, Y.; Suzuki, T.; Taga, Y. *Appl. Phys. Lett.* **2001**, *79*, 156; (c) Baldo, M. A.; Lamansky, S.; Burrows, P. E.; Thompson, M. E.; Forrest, S. R. *Appl. Phys. Lett.* **1999**, *75*, 4.
3. (a) Burroughes, J. H.; Bradley, D. D. C.; Brown, A. R.; Marks, R. N.; Mackay, K.; Friend, R. H.; Burn, P. L.; Holmes, A. B. *Nature* **1990**, *347*, 539; (b) Lo, S.-C.; Burn, P. L. *Chem. Rev.* **2007**, *107*, 1097; (c) Burn, P. L.; Lo, S.-C.; Samuel, I. D. W. *Adv. Mater.* **2007**, *19*, 1675.
4. (a) Giebink, N. C.; D'Andrade, B. W.; Weaver, M. S.; Brown, J. J.; Forrest, S. R. *J. Appl. Phys.* **2009**, *105*, 124514; (b) Sivasubramaniam, V.; Brodkorb, F.; Hanning, S.; Buttler, O.; Loebl, H. P.; van Elsbergen, V.; Boerner, H.; Scherf, U.; Kreyenschmidt, M. *Solid State Sci.* **2009**, *11*, 1933; (c) Chang, J.; Yu, Y.-J.; Na, J. H.; An, J.; Im, C.; Choi, D.-H.; Jin, J.-I.; Lee, S. H.; Kim, Y. K. J. *Polym. Sci., Part B: Polym. Phys.* **2008**, *46*, 2395; (d) Giebink, N. C.; D'Andrade, B. W.; Weaver, M. S.; Mackenzie, P. B.; Brown, J. J.; Thompson, M. E.; Forrest, S. R. *J. Appl. Phys.* **2008**, *103*, 044509; (e) So, F.; Kondakov, D. *Adv. Mater.* **2010**, *22*, 3762.
5. (a) Webster, G. R.; Mitchell, W. J.; Burn, P. L.; Thomas, R. K.; Fragneto, G.; Markham, J. P. J.; Samuel, I. D. W. *J. Appl. Phys.* **2002**, *91*, 9066; (b) Mitchell, W. J.; Burn, P. L.; Thomas, R. K.; Fragneto, G. *Appl. Phys. Lett.* **2003**, *82*, 2724; (c) Mitchell, W. J.; Burn, P. L.; Thomas, R. K.; Fragneto, G.; Markham, J. P. J.; Samuel, I. D. W. *J. Appl. Phys.* **2004**, *95*, 2391; (d) Jukes, P. C.; Martin, S. J.; Higgins, A. M.; Geoghegan, M.; Jones, R. A. L.; Langridge, S.; Wehrum, A.; Kirchmeyer, S. *Adv. Mater.* **2004**, *16*, 807; (e) Higgins, A. M.; Cadby, A.; Lidzey, D. C.; Dalgliesh, R. M.; Geoghegan, M.; Jones, R. A. L.; Martin, S. J.; Heriot, S. Y. *Adv. Funct. Mater.* **2009**, *19*, 157; (f) Vickers, S. V.; Barcena, H.; Knights, K. A.; Thomas, R. K.; Ribierre, J.-C.; Gambino, S.; Samuel, I. D. W.; Burn, P. L.; Fragneto, G. *Appl. Phys. Lett.* **2010**, *96*, 263302; (g) Cavaye, H.; Smith, A.; James, M.; Nelson, A.; Burn, P. L.; Gentle, I. R.; Meredith, P. *Langmuir* **2009**, *25*, 12800; (h) Smith, A. R. G.; Ruggles, J. L.; Cavaye, H.; Shaw, P.; Darwish, T. A.; James, M.; Gentle, I. R.; Burn, P. L. *Adv. Funct. Mater.* **2011**, *21*, 2225; (i) Lee, K. H.; Schwenn, P. E.; Smith, A. R. G.; Cavaye, H.; Shaw, P. E.; James, M.; Kruger, K.; Meredith, P.; Gentle, I. R.; Burn, P. L. *Adv. Mater.* **2011**, *23*, 766; (j) Tong, C. C.; Hwang, K. C. *J. Phys. Chem. C* **2007**, *111*, 3490; (k) Abe, T.; Miyazawa, A.; Konno, H.; Kawanishi, Y. *Chem. Phys. Lett.* **2010**, *491*, 199; (l) Cavaye, H.; Shaw, P. E.; Smith, A. R. G.; Burn, P. L.; Gentle, I. R.; James, M.; Lo, S.-C.; Meredith, P. *J. Phys. Chem. C* **2011**, *115*, 18366.
6. Hawthorne, S. B.; Miller, D. J.; Aulich, T. R.; Fresenius, Z. *Anal. Chem.* **1989**, *334*, 421.
7. (a) Atzrodt, J.; Derdau, V.; Fey, T.; Zimmermann, J. *Angew. Chem. Int. Ed.* **2007**, *46*, 7744; (b) Derdau, V.; Atzrodt, J.; Zimmermann, J.; Kroll, C.; Brückner, F. *Chem. Eur. J.* **2009**, *15*, 10397; (c) Atzrodt, J.; Derdau, V. *J. Labelled Compd. Radiopharm.* **2010**, *53*, 674.
8. (a) Sajiki, H.; Aoki, F.; Esaki, H.; Maegawa, T.; Hirota, K. *Org. Lett.* **2004**, *6*, 1485; (b) Sajiki, H.; Esaki, H.; Aoki, F.; Maegawa, T.; Hirota, K. *Synlett* **2005**, 1385; (c) Esaki, H.; Aoki, F.; Maegawa, T.; Hirota, K.; Sajiki, H. *Heterocycles* **2005**, *66*, 361; (d) Maegawa, T.; Akashi, A.; Esaki, H.; Aoki, F.; Sajiki, H.; Hirota, K. *Synlett* **2005**, 845; (e) Esaki, H.; Ito, N.; Sakai, S.; Maegawa, T.; Monguchi, Y.; Sajiki, H. *Tetrahedron* **2006**, *62*, 10954; (f) Esaki, H.; Aoki, F.; Umemura, M.; Kato, M.; Maegawa, T.; Monguchi, Y.; Sajiki, H. *Chem. Eur. J.* **2007**, *13*, 4052; (g) Kurita, T.; Hattori, K.; Seki, S.; Mizumoto, T.; Aoki, F.; Yamad, Y.; Ikawa, K.; Maegawa, T.; Monguchi, Y.; Sajiki, H. *Chem. Eur. J.* **2008**, *14*, 664; (h) Ito, N.; Esaki, H.; Maesawa, T.; Imamiya, E.; Maegawa, T.; Sajiki, H. *Bull. Chem. Soc. Jpn.* **2008**, *81*, 278; (i) Sajiki, H.; Ito, N.; Esaki, H.; Maesawa, T.; Maegawa, T.; Hirota, K. *Tetrahedron Lett.* **2005**, *46*, 6995; (j) Ito, N.; Watahiki, T.; Maesawa, T.; Maegawa, T.; Sajiki, H. *Adv. Synth. Catal.* **2006**, *348*, 1025.
9. (a) Jameson, C. J. In *Isotopes in the Physical and Biomedical Sciences*; Elsevier Science Publishers: Amsterdam, 1991; Vol. 2, p. 1; (b) Jameson, C. J.; Osten, H. J. *Ann. Rep. NMR Spectrosc.* **1986**, *17*, 1; (c) Jameson, C. J.; Osten, H. J. *J. Am. Chem. Soc.* **1985**, *107*, 4158.
10. Liu, Q.; Lu, J.; Ding, J.; Day, M.; Tao, Y.; Barrios, P.; Stupak, J.; Chan, K.; Li, J.; Chi, Y. *Adv. Funct. Mater.* **2007**, *17*, 1028.
11. (a) James, M. A.; Nelson, A.; Brule, J. C.; Schulz, J. *Neutron Res.* **2006**, *14*, 91; (b) James, M.; Nelson, A.; Holt, S. A.; Saerbeck, T.; Hamilton, W. A.; Klose, F. *Nucl. Instrum. Methods Phys. Res. A* **2011**, *632*, 112.
12. (a) Nelson, A. *J. Appl. Crystallogr.* **2006**, *39*, 273; (b) Nelson, A. *J. Phys.: Conf. Ser.* **2010**, *251*, 012094.